

Durham Research Online

Deposited in DRO:

22 May 2015

Version of attached file:

Published Version

Peer-review status of attached file:

Peer-reviewed

Citation for published item:

Lacey, Cedric G. (1988) 'The structure of shocks with thermal conduction and radiative cooling.',
Astrophysical journal., 326 . pp. 769-778.

Further information on publisher's website:

<http://dx.doi.org/10.1086/166136>

Publisher's copyright statement:

© 1988. The American Astronomical Society. All rights reserved. Printed in the U.S.A.

Additional information:

Use policy

The full-text may be used and/or reproduced, and given to third parties in any format or medium, without prior permission or charge, for personal research or study, educational, or not-for-profit purposes provided that:

- a full bibliographic reference is made to the original source
- a [link](#) is made to the metadata record in DRO
- the full-text is not changed in any way

The full-text must not be sold in any format or medium without the formal permission of the copyright holders.

Please consult the [full DRO policy](#) for further details.

THE STRUCTURE OF SHOCKS WITH THERMAL CONDUCTION AND RADIATIVE COOLING

CEDRIC G. LACEY

Harvard-Smithsonian Center for Astrophysics and Princeton University Observatory

Received 1987 June 15; accepted 1987 September 14

ABSTRACT

A general analysis is presented of the structure of a steady state, plane-parallel shock wave in which both thermal conduction and radiative cooling are important. The fluid is assumed to have a perfect-gas equation of state, with radiative cooling a function only of its temperature and density. Conduction in both diffusive and saturated regimes is treated. For the case of a strong shock, with conductivity and cooling function varying as power laws in temperature, approximate analytic solutions describing the shock wave are derived. For a plasma of solar composition, conduction is found to have a significant effect on the shock temperature and overall thickness of the postshock layer only for shock velocities $v_0 \gtrsim 3 \times 10^4 \text{ km s}^{-1}$, corresponding to shock temperatures $T_s \gtrsim 10^{10} \text{ K}$, but it affects the local structure of parts of the shock wave at much lower velocities. The effects of conduction are greatly enhanced if the heavy-element abundance is increased.

Subject headings: hydrodynamics — shock waves

I. INTRODUCTION

Considerable work has been devoted to the effects of heat conduction on the interface between a hot gas and a cold gas in the case that approximate pressure equilibrium holds throughout the fluid, with all flows being subsonic. If there is no radiative cooling, a thermal wave propagates from the hot gas into the cold gas, evaporating the cold phase (e.g., Zel'dovich and Raizer 1967). If there is radiative cooling, the behavior is more complicated (e.g., Doroshkevich and Zel'dovich 1981): if the boundary between the phases is initially infinitely sharp, then at early times a thermal wave propagates into the cold phase, and there is evaporation, but at late times a cooling wave propagates into the hot phase, and there is condensation onto the cold phase (this discussion assumes that the cooling time scale for the hot gas exceeds that for cooler gas, as is typically the case). These ideas have been applied to the evaporation of clouds in the interstellar medium (e.g., Penston and Brown 1970; Cowie and McKee 1977; McKee and Cowie 1977).

In the opposite extreme, one has the case that there is a large pressure difference between two bodies of gas, and the interface propagates as a shock front moving supersonically into the low-pressure gas. There has been extensive work on the separate effects on shock waves of thermal conduction (reviewed by Zel'dovich and Raizer 1967) and radiative cooling (reviewed by McKee and Hollenbach 1980), but no systematic investigation of their combined effects. Chevalier (1975) and Cowie (1977) investigated (mainly by means of time-dependent numerical simulations) the effects of thermal conduction on the evolution of supernova remnants, in which a point explosion drives a roughly spherical shock into the surrounding medium. More recently, Bond *et al.* (1984) and Shapiro and Struck-Marcell (1985) have performed time-dependent numerical simulations of the planar shock structures arising from gravitational collapse in the "pancake" theory of galaxy formation, including both radiative cooling and thermal conduction. While assuming similar physical parameters, Bond *et al.* and Shapiro and Struck-Marcell come to opposite conclusions about the effects of thermal conductivity on their results.

In view of this, it seemed worthwhile to make a more systematic investigation of the structure of shocks with both radiative cooling and thermal conduction, to elucidate the conditions under which thermal conduction is likely to be an important

effect. An additional motivation was that (with the exception of some of the numerical simulations referred to) previous investigations of the effects of thermal conduction had all assumed that the heat flux was given by the diffusive approximation $Q = -\kappa(T) dT/dx$, valid when the mean free path of the particles transporting the energy is small compared with the length scale of temperature variation. This approximation breaks down when the temperature gradient becomes very large, and the heat flux saturates at a value Q_{sat} independent of $|dT/dx|$, as discussed, for instance, by Cowie and McKee (1977).

The investigations in this paper are restricted to shocks in plane-parallel, steady state flows. In addition, I assume that the gas may be treated as a single fluid with a perfect-gas equation of state, although for an ionized gas a two-fluid treatment, with the electrons and ions allowed to have different temperatures, would be more exact. I assume equilibrium radiative cooling, in which the cooling rate depends only on the present temperature and density of the gas. The plan of the paper is as follows: Section II gives the basic equations of steady, one-dimensional gas flow. These are cast into dimensionless form. For the case in which the thermal conductivity and radiative cooling rate per unit volume have the dependences $\kappa = \kappa(T)$ and $\Lambda = \rho^2 \bar{L}(T)$, the solutions scale straightforwardly with the density. Section III outlines a general procedure for solving the steady-flow equations and gives a qualitative description of the behaviors produced by radiative cooling, thermal conduction, and flux saturation. Section IV derives approximate analytic solutions for the shock temperature and for the structure of the pre- and postshock regions in a strong shock wave, assuming that the conductivity and cooling rate vary as power laws in temperature. Section V presents results for the astrophysically interesting case of a fully ionized plasma, with heat conduction by free electrons and cooling by bremsstrahlung and line and recombination radiation. Estimates are given for the shock velocity at which conduction becomes important. Section VI is a summary.

II. BASIC EQUATIONS

We consider the one-dimensional steady flow of a non-viscous gas. In the frame in which the shock front is at rest, the equations of mass conservation, momentum conservation, and

energy balance are (e.g., Landau and Lifshitz 1959):

$$\frac{d}{dx}(\rho v) = 0, \quad (2.1a)$$

$$\frac{d}{dx}(p + \rho v^2) = 0, \quad (2.1b)$$

$$\frac{d}{dx} \left[\rho v \left(\frac{1}{2} v^2 + h \right) + Q \right] = -\Lambda, \quad (2.1c)$$

where v (>0) is the velocity; ρ , p , T , h are respectively the density, pressure, temperature, and enthalpy per unit mass; Q is the heat flux due to conduction; and Λ is the radiative cooling rate per unit volume. The shock wave is assumed to be optically thin to its own radiation. We specialize to the case of a perfect gas with adiabatic index $\gamma = 5/3$ and (constant) mean molecular mass μ , for which $p = (k_B/\mu m_H)\rho T$. It is convenient to introduce a scaled temperature variable defined by

$$\bar{T} \equiv k_B T / \mu m_H = p / \rho, \quad (2.2)$$

in terms of which

$$h = \frac{5}{2} \bar{T}; \quad (2.3)$$

\bar{T} is the square of the isothermal sound speed.

Equations (2.1a) and (2.1b) can be integrated immediately. We assume that far upstream ($x \rightarrow -\infty$, for $v > 0$), the pressure, density, and velocity are p_0 , ρ_0 , and v_0 . Then

$$\rho v = \rho_0 v_0, \quad (2.4)$$

$$p + \rho v^2 = p_0 + \rho_0 v_0^2. \quad (2.5)$$

We define an energy flux

$$F \equiv \rho_0 v_0 \left(\frac{1}{2} v^2 + \frac{5}{2} \bar{T} \right) + Q, \quad (2.6)$$

in terms of which equation (2.1c) becomes

$$\frac{dF}{dx} = -\Lambda(\rho, T). \quad (2.7)$$

The above equations apply in regions of the flow where the flow variables are all continuous. At a shock front, where ρ and v vary discontinuously, they must be supplemented by jump conditions relating flow variables on either side of the discontinuity ($[X]$ denotes the change in X across the shock discontinuity, moving in the flow direction):

$$[\rho v] = 0, \quad (2.8a)$$

$$[p + \rho v^2] = 0, \quad (2.8b)$$

$$[F] = 0. \quad (2.8c)$$

Equations (2.8a) and (2.8b) are in fact equivalent to equations (2.4) and (2.5), respectively, while equation (2.8c) can be derived by integrating equation (2.7) across the shock discontinuity (Λ being everywhere finite). The solution to the flow is found by integrating equation (2.7), in conjunction with equations (2.4) and (2.5), and the jump condition (2.8c). For some purposes it is convenient to use as the independent variable the column density rather than the spatial coordinate; they are related by

$$\Sigma \equiv \int \rho dx. \quad (2.9)$$

We have yet to specify the form of the conductive heat flux Q and the radiative cooling rate Λ . For small temperature gra-

dients, the conductive flux is given by the diffusion approximation: $Q_{\text{diff}} = -\kappa(\rho, T)dT/dx = -\bar{\kappa}(\rho, \bar{T})d\bar{T}/dx$, but for large temperature gradients the heat flux saturates at a value Q_{sat} independent of $|dT/dx|$ (e.g., Cowie and McKee 1977). On dimensional grounds, Q_{sat} must vary as the product of the thermal energy density with the typical thermal velocity; thus $Q_{\text{sat}} = -\bar{\theta}\rho\bar{T}^{3/2} \text{sgn}(d\bar{T}/dx)$, with $\bar{\theta}$ dimensionless. $\bar{\theta}$ is related to Cowie and McKee's ϕ_s parameter by $\bar{\theta} = 5\phi_s$. The actual conductive flux will be assumed to be the minimum of the diffusive and saturated fluxes:

$$Q = -\min(\bar{\kappa}|d\bar{T}/dx|, \bar{\theta}\rho\bar{T}^{3/2}) \text{sgn}(d\bar{T}/dx). \quad (2.10)$$

Where needed, the conductivity and the radiative cooling rate will be assumed to have the dependences $\bar{\kappa} = \bar{\kappa}(\bar{T})$ and $\Lambda = \rho^2 \bar{L}(\bar{T})$, as usually occurs in practice, with $\bar{L} = 0$ for $T < T_c$.

a) Dimensionless Form of Equations

For the purpose of solving the flow equations, it is convenient to introduce dimensionless flow variables (cf. Zel'dovich and Raizer 1967). Define a dimensionless velocity

$$\eta \equiv v/v_0. \quad (2.11)$$

Combining with equation (2.4), we have

$$\rho = \rho_0/\eta. \quad (2.12)$$

Define a dimensionless temperature

$$\tau \equiv \bar{T}/v_0^2 = \eta(1 + \tau_0 - \eta), \quad (2.13)$$

where the second equality follows from equations (2.5), (2.11), and (2.12). The initial temperature τ_0 is related to the adiabatic Mach number M of the shock: $M^2 \equiv (v_0/c_0)^2 = \frac{3}{5}\tau_0^{-1}$, where $c_0 = (5p_0/3\rho_0)^{1/2}$ is the adiabatic sound speed. For a shock, we have the condition $M > 1$; thus $\tau_0 < \frac{3}{5}$. We define a dimensionless spatial coordinate ξ , and dimensionless total and conductive energy fluxes f and q :

$$\xi = x/x_0, \quad (2.14)$$

$$f \equiv \frac{F}{\frac{1}{2}\rho_0 v_0^3} = 4\eta \left[\frac{5}{4}(1 + \tau_0) - \eta \right] + q, \quad (2.15)$$

$$q \equiv \frac{Q}{\frac{1}{2}\rho_0 v_0^3} = -\min \left[k(\tau) \left| \frac{d\tau}{d\xi} \right|, \frac{2\bar{\theta}\tau^{3/2}}{\eta} \right] \text{sgn} \left(\frac{d\tau}{d\xi} \right), \quad (2.16)$$

where

$$k(\tau) \equiv \frac{2\bar{\kappa}(\bar{T})}{\rho_0 x_0 v_0}. \quad (2.17)$$

It is also convenient to define

$$g(\eta) \equiv 4\eta \left[\frac{5}{4}(1 + \tau_0) - \eta \right] \quad (2.18)$$

as the component of the dimensionless energy flux due to the motion of the fluid. Thus the total energy flux is $f = g + q$.

For $\Lambda = \rho^2 \bar{L}(\bar{T})$, the energy-balance equation (2.7) becomes

$$\frac{df}{d\xi} = -\frac{l(\tau)}{\eta^2}, \quad (2.19)$$

where

$$l(\tau) \equiv \frac{2\rho_0 x_0 \bar{L}(\bar{T})}{v_0^3}. \quad (2.20)$$

In the above, x_0 is some characteristic length scale for the

shock layer, based on the conductivity or the cooling function, that we have still to specify. We are free to define x_0 so that it has the scaling $x_0 \propto 1/\rho_0$, so that ρ_0 disappears from the problem except as an overall scaling factor. These equations can easily be generalized to the case in which $\Lambda(\rho, T)$ has a different form, or $\bar{\kappa} = \bar{\kappa}(\rho, T)$, but then the solutions no longer scale in a simple way with ρ_0 . The dimensionless column density is

$$\sigma \equiv \Sigma/\rho_0 x_0 = \int (1/\eta) d\xi. \quad (2.21)$$

III. SOLUTION OF SHOCK STRUCTURE

The initial, upstream ($\xi \rightarrow -\infty$) state of the gas is $\eta = 1$, $\tau = \tau_0 < \frac{3}{5}$, and the final, downstream ($\xi \rightarrow \infty$) state is $\eta = \eta_1 < 1$, $\tau = \tau_1 \equiv \eta_1(1 + \tau_0 - \eta_1)$. In the initial and final states, $d\eta/d\xi = 0$, $q = 0$, $l = 0$. The function $\eta(\xi)$ decreases monotonically from the initial to the final states, $d\eta/d\xi \leq 0$, and varies discontinuously at a shock. We assume that the radiative cooling function has $l(\tau) = 0$ for $\tau < \tau_c$, so, for the initial and final states to be equilibria, we must have $\tau_0 \leq \tau_c$, $\tau_1 \leq \tau_c$. The total energy flux decreases monotonically and continuously, $df/d\xi \leq 0$, so that $f_1 \leq f_0 = 1 + 5\tau_0$. In the initial and final

states, $f = 4\eta[\frac{3}{4}(1 + \tau_0) - \eta]$ (eq. [2.15]), so the bound on f_1 gives $\eta_1 \leq \frac{3}{4}(1 + 5\tau_0)$. In the absence of cooling, $f_1 = f_0$, $\eta_1 = \frac{3}{4}(1 + 5\tau_0)$, $\tau_1 = \frac{1}{16}(1 + 5\tau_0)(3 - \tau_0)$, and $\tau_0 \leq \tau(\xi) \leq \tau_1$. The condition that cooling not occur is simply $\tau_c > \frac{1}{16}(1 + 5\tau_0)(3 - \tau_0)$. In the case $\tau_c < \frac{1}{16}(1 + 5\tau_0)(3 - \tau_0)$, the gas radiates energy, and the final state is $\eta_1 = \eta_c$, $\tau_1 = \tau_c$, where

$$\eta_c \equiv \frac{1}{2}(1 + \tau_0) - [\frac{1}{4}(1 + \tau_0)^2 - \tau_c]^{1/2} \quad (3.1)$$

is the smaller root of equation (2.13) for $\tau = \tau_c$.

a) Solution for Unsaturated Conduction

We assume for the present that the conductive heat flux is everywhere unsaturated (formally, we let $\bar{\theta} \rightarrow \infty$), and postpone discussion of the effects of saturation to the next section. In this case,

$$q = q_{\text{diff}} \equiv -k(\tau)d\tau/d\xi; \quad (3.2)$$

q must be finite everywhere, since f is, so $\tau(\xi)$ must be continuous, even at shocks. Consider the solution trajectory in the τ - η plane. There are four cases to consider, depending on the values of τ_0 and τ_c (they are sketched in Fig. 1):

1. $\tau_0 > \frac{3}{5}$, $\tau_c > \frac{1}{16}(1 + 5\tau_0)(3 - \tau_0)$: η and τ vary contin-

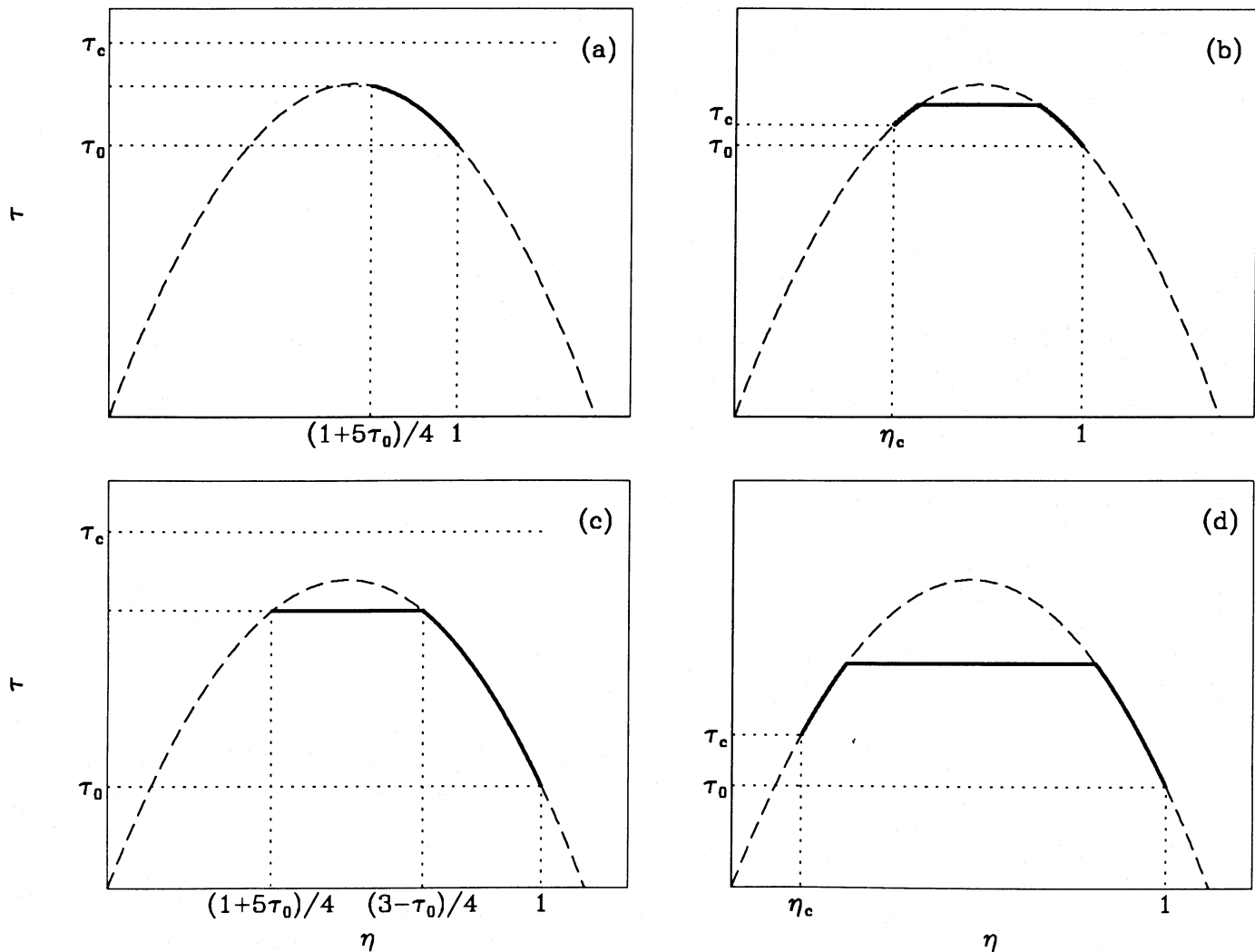


FIG. 1.—Trajectories in τ - η plane for various values of τ_0 and τ_c . Solid curve shows actual trajectory; dashed curve shows $\tau(\eta)$ relation. See text for details.

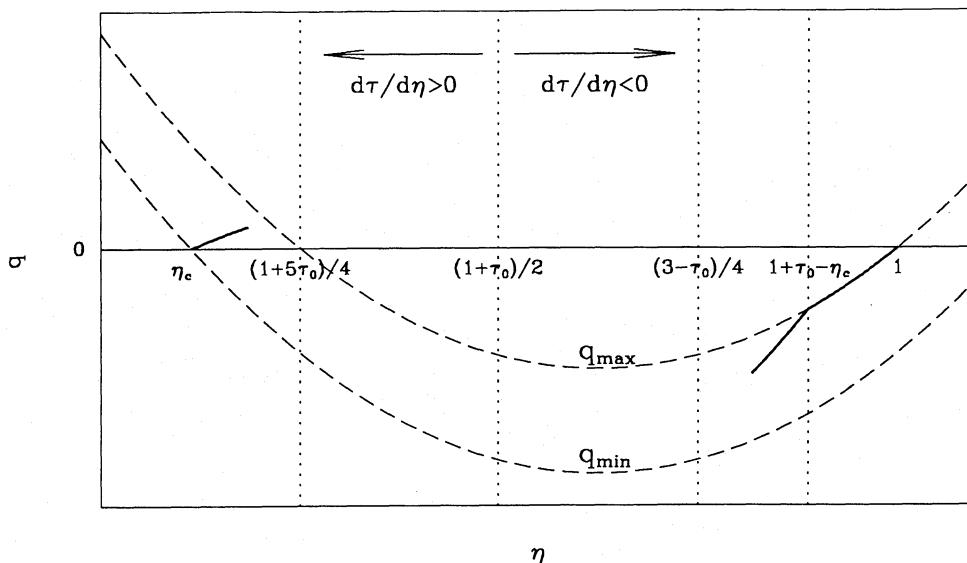


FIG. 2.—Trajectory in q - η plane. Solid curve shows actual trajectory (discontinuous at shock); dashed curves show bounds on q . See text for details.

uously, with no jump. The final state is $\eta_1 = \frac{1}{4}(1 + 5\tau_0)$ (Fig. 1a).

2. $\tau_0 > \frac{1}{3}$, $\tau_c < \frac{1}{16}(1 + 5\tau_0)(3 - \tau_0)$: η has a shock jump. The final state is $\eta = \eta_c$, $\tau = \tau_c$ (Fig. 1b).

3. $\tau_0 < \frac{1}{3}$, $\tau_c > \frac{1}{16}(1 + 5\tau_0)(3 - \tau_0)$: η has a jump. The final state is $\eta_1 = \frac{1}{4}(1 + 5\tau_0)$ (Fig. 1c).

4. $\tau_0 < \frac{1}{3}$, $\tau_c < \frac{1}{16}(1 + 5\tau_0)(3 - \tau_0)$: η has a jump. The final state is $\eta = \eta_c$, $\tau = \tau_c$ (Fig. 1d).

For the nonradiative case, the reason why a jump in η occurs for $\tau_0 < \frac{1}{3}$ ($M^2 > 9/5$) is as follows (Zel'dovich and Raizer 1967): The form of the $\tau(\eta)$ relation (eq. [2.13]), together with the assumption $d\eta/d\xi \leq 0$, requires $d\tau/d\xi \geq 0$ and thus $q \leq 0$ for $\eta > \frac{1}{2}(1 + \tau_0)$, and $d\tau/d\xi \leq 0$, $q \geq 0$ for $\eta < \frac{1}{2}(1 + \tau_0)$. On the other hand, energy conservation (eq. [2.15]) with $f = f_0$ requires $q > 0$ for $\eta > \frac{1}{4}(1 + 5\tau_0)$, and vice versa. Therefore, it is impossible for the solution to evolve continuously through the range $\frac{1}{4}(1 + 5\tau_0) < \eta < \frac{1}{2}(1 + \tau_0)$. Since τ must vary continuously, the solution jumps from $\eta = \frac{1}{4}(3 - \tau_0)$ to $\eta = \frac{1}{4}(1 + 5\tau_0)$.

This argument can be generalized to the radiative case: f is then bounded between its initial and final values, $f_1 \leq f \leq f_0$, and q correspondingly has bounds depending on η : $q_{\min}(\eta) \leq q(\eta) \leq q_{\max}(\eta)$, where $q_{\min}(\eta) \equiv f_1 - g(\eta)$, $q_{\max}(\eta) \equiv f_0 - g(\eta)$. Again we find that for $\tau_0 < \frac{1}{3}$, the solution cannot vary continuously in the range $\frac{1}{4}(1 + 5\tau_0) < \eta < \frac{1}{2}(1 + \tau_0)$, and so must jump across the range $\frac{1}{4}(1 + 5\tau_0) < \eta < \frac{1}{4}(3 - \tau_0)$. A sketch of the behavior for this case is given in Figure 2.

In the case that the shock is radiative, the location in η of the shock jump is not known *a priori*, and must be found by integrating the energy equation inward (toward the shock) from the initial and final states and matching at some intermediate point. It is convenient to perform this matching in the f - τ plane; $f(\xi)$ and $\tau(\xi)$ are both continuous, and thus $f(\tau)$ is also continuous. It is, however, in general double-valued because $\tau(\eta)$ has two roots for each value of τ in the range $\tau < \frac{1}{4}(1 + \tau_0)^2$: there is a branch $f_+(\tau)$ corresponding to the range $\eta > \frac{1}{2}(1 + \tau_0)$ and a branch $f_-(\tau)$ for the range $\eta < \frac{1}{2}(1 + \tau_0)$. The monotonicity conditions $df_+/d\tau \leq 0$, $df_-/d\tau \geq 0$ follow from $df/d\xi \leq 0$. The location of the shock $\tau = \tau_s$ is given by the intersection of $f_+(\tau)$ and $f_-(\tau)$, as is sketched in Figure 3. Then

$f_{\pm}(\tau)$ can be calculated as follows: Dividing equation (2.19) by equation (3.2) results in

$$\frac{df}{d\tau} = \frac{k(\tau)l(\tau)}{\eta^2 q}. \quad (3.3)$$

Combining this with equations (2.13) and (2.15) then gives a differential equation for $q(\eta)$:

$$\frac{dq^2}{d\eta} + 2[5(1 + \tau_0) - 8\eta]q = \frac{2(1 + \tau_0 - 2\eta)k(\tau)l(\tau)}{\eta^2}, \quad (3.4)$$

which can be integrated from $\eta = 1$ and $\eta = \eta_c$ in the directions of decreasing and increasing η , respectively. From $q(\eta)$ one derives $f(\eta) = g(\eta) + q(\eta)$, and thus $f_{\pm}(\tau)$. Note that the trajectories in the f - τ plane depend on the conductivity and cooling function only through the product $k(\tau)l(\tau) = 4\bar{\kappa}(\bar{T})\bar{L}(\bar{T})/v_0^4$. Once the location of the shock has been solved for, the spatial

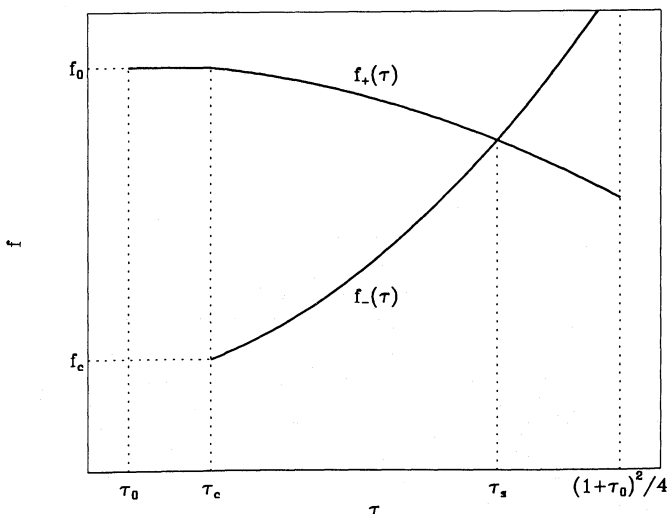


FIG. 3.—Matching of trajectories in f - τ plane to determine shock temperature τ_s .

dependence of the fluid variables can be found by integrating

$$\frac{d\xi}{d\eta} = \eta \frac{d\sigma}{d\eta} = -\frac{(1 + \tau_0 - 2\eta)k(\tau)}{q(\eta)} \quad (3.5)$$

to give $\xi(\eta)$ or $\sigma(\eta)$, and then inverting, to give $\eta(\xi)$, $\tau(\xi)$, and so on.

b) Solution for Saturated Conduction

In the case in which $\bar{\theta}$ is finite, the conductive flux is limited by the condition $|q| \leq |q_{\text{sat}}(\eta)|$, where

$$q_{\text{sat}} = -2\bar{\theta}\eta^{1/2}(1 + \tau_0 - \eta)^{3/2} \text{sgn}(d\tau/d\xi). \quad (3.6)$$

An immediate consequence is that $\tau(\xi)$ no longer need be continuous, since q remains finite even if $d\tau/d\xi$ is infinite. Therefore solution trajectories in the f - τ plane may make horizontal jumps across certain ranges of τ . The condition $|q| = |q_{\text{sat}}(\eta)|$ defines unique trajectories (independent of $\bar{\kappa}(\bar{T})$ and $\bar{L}(\bar{T})$) for the (+) and (-) branches of $f(\tau)$:

$$f_{+\text{sat}}(\eta) = g(\eta) - |q_{\text{sat}}(\eta)|, \quad (3.7a)$$

$$f_{-\text{sat}}(\eta) = g(\eta) + |q_{\text{sat}}(\eta)|. \quad (3.7b)$$

For a solution trajectory coinciding with $f = f_{\text{sat}}$, $\xi(\eta)$ can be found by integrating

$$\frac{d\xi}{d\eta} = -\frac{\eta^2 df_{\text{sat}}/d\eta}{l(\tau)}. \quad (3.8)$$

The condition $|q| \leq |q_{\text{sat}}|$ translates into bounds on $f_{\pm}(\tau)$: $f_{+\text{sat}}(\tau) \leq f_+(\tau) \leq g_+(\tau)$, $g_-(\tau) \leq f_-(\tau) \leq f_{-\text{sat}}(\tau)$, where $g_{\pm}(\tau)$ denotes $g(\eta)$ evaluated on the (+) or (-) branches of $\eta(\tau)$. The function $g_+(\tau)$ has a maximum in the range $0 < \tau < \frac{1}{4}(1 + \tau_0)^2$, and $f_{+\text{sat}}(\tau)$ also has a maximum, if $\bar{\theta}$ is sufficiently small, as is sketched in Fig. 4a. For larger $\bar{\theta}$, $f_{+\text{sat}}(\tau)$ is monotonically decreasing, as is shown in Figure 4b. The function $g_-(\tau)$ monotonically increases, and so does $f_{-\text{sat}}(\tau)$ in the range $0 < \tau < \frac{1}{4}(1 + \tau_0)^2$, $0 < f < f_0$ (the latter restriction being necessary because $|q_{\text{sat}}|$ has a maximum), as shown in Figure 4c.

Consider the behavior of $f_+(\tau)$, integrating inward from $\tau = \tau_0$. At $\tau = \tau_0$, $q = 0$, while $|q_{\text{sat}}| > 0$ if $\bar{\theta} > 0$, $\tau_0 > 0$, so the solution is initially unsaturated. At some point, the solution $f_+(\tau)$ found via integration of equation (3.4) may intersect the curve $f = f_{+\text{sat}}(\tau)$. The subsequent behavior depends on whether $df_{+\text{sat}}/d\tau > 0$ or < 0 at the intersection. If $df_{+\text{sat}}/d\tau >$

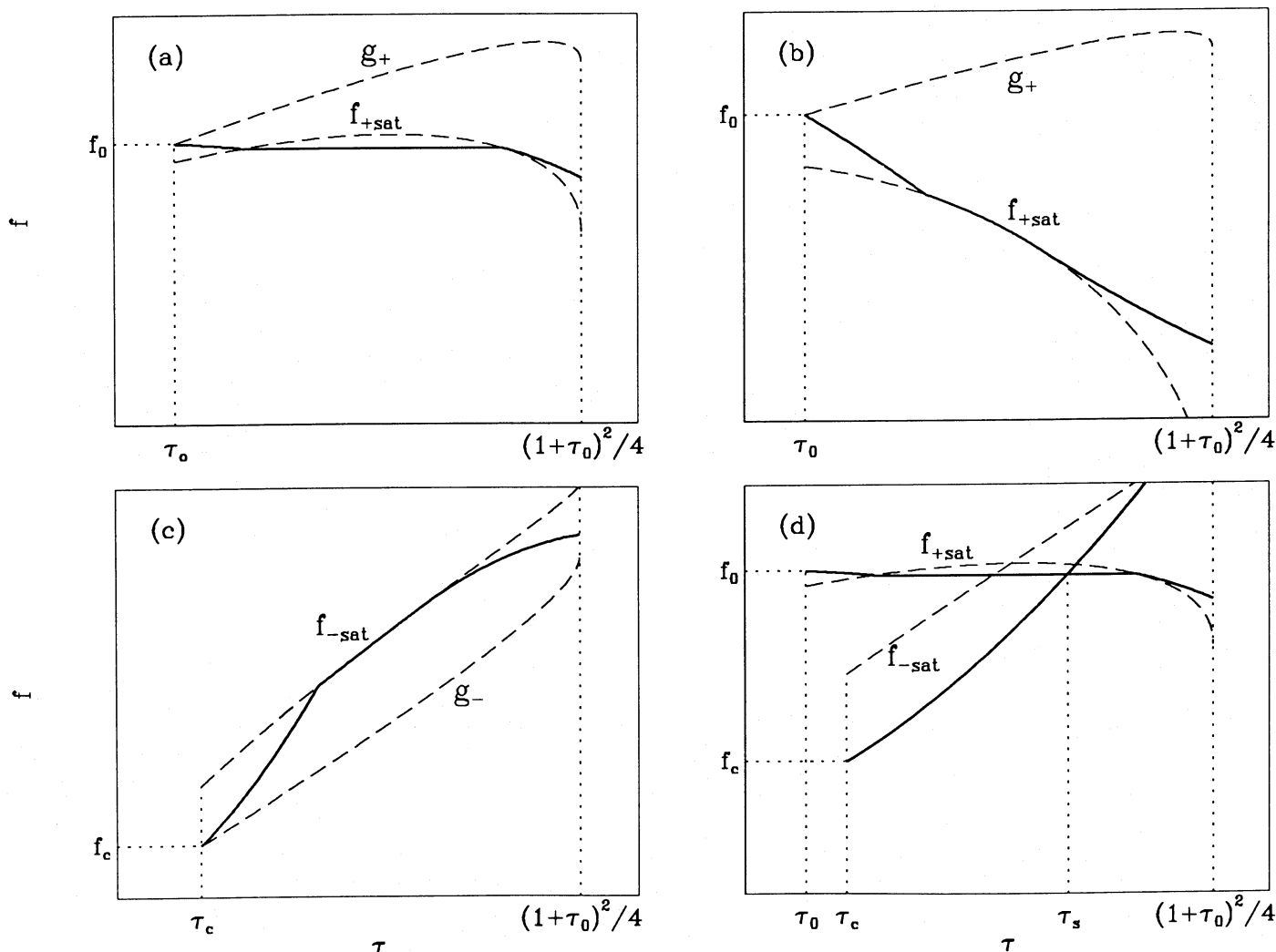


FIG. 4.—Effects of conductive saturation on trajectories in f - τ plane. Solid curves show actual trajectories; dashed curves show bounds on f . See text for details.

0, the solution must jump across to the point on the f_{+sat} curve with the same value of f , since f cannot increase. There results a shock discontinuity at which there are jumps in both temperature and density. This case is sketched in Figure 4a. If $df_{+sat}/d\tau < 0$, then the solution is forced to follow the $f = f_{+sat}$ curve in the direction of increasing τ for as long as $df_{+unsat}/d\tau < df_{+sat}/d\tau$ along this curve, where $df_{+unsat}/d\tau$ is evaluated via equation (3.4) as though the conduction were unsaturated. This case is sketched in Figure 4b. The solution can branch off again from $f = f_{+sat}$ if it reaches a point where $df_{+unsat}/d\tau = df_{+sat}/d\tau$ and $(d/d\tau)(df_{+unsat}/d\tau - df_{+sat}/d\tau) > 0$.

The behavior of $f_{-}(\tau)$ is similar, except that intersection of $f_{-}(\tau)$ with $f_{-sat}(\tau)$ does not result in a shock discontinuity because $df_{-sat}/d\tau \geq 0$. The solution is forced to follow $f = f_{-sat}(\tau)$ (moving in the direction of increasing τ) for as long as $df_{-unsat}/d\tau > df_{-sat}/d\tau$, as sketched in Figure 4c. It can branch off again where $df_{-unsat}/d\tau = df_{-sat}/d\tau$ and $(d/d\tau)(df_{-unsat}/d\tau - df_{-sat}/d\tau) < 0$. Again, the shock location is found from the intersection of $f_{+}(\tau)$ and $f_{-}(\tau)$. In the case in which $f_{+}(\tau)$ has a jump, the intersection may occur in the jump region, as sketched in Figure 4d.

c) Spatial Structure of Shock

Combining the results of §§ IIIa and IIIb, we can give a qualitative picture of the spatial structure of the transition region between the upstream and downstream states. Neglecting saturation, one finds an isothermal shock, at which $\tau = \tau_s$, and η jumps from η_{s-} to η_{s+} , if either $\tau_0 < \frac{1}{3}$ or $\tau_0 < \tau_c < \frac{1}{16}(1 + 5\tau_0)(3 - \tau_0)$ for $\tau_0 < \frac{3}{5}$. We define $\xi = 0$ at this "main shock." The temperature τ_s at the shock is the maximum temperature achieved in the flow. If there is no radiative cooling, the postshock flow is at constant temperature. Radiative cooling causes the temperature to decline from τ_s to τ_c beyond the shock. A conductive precursor propagates ahead of the main shock, in the region $\xi < 0$ where $\eta_{s-} < \eta < 1$. If the conduction is everywhere unsaturated, then the temperature in this precursor increases continuously from $\tau = \tau_0$ upstream to $\tau = \tau_s$ at the shock. If $k(\tau) \rightarrow 0$ as $\tau \rightarrow \tau_0$, the precursor extends only a finite distance ahead of the shock.

When saturation effects are included, there may be an additional "precursor shock" ahead of the main shock at $\xi = \xi_p < 0$, at which τ jumps from τ_{p-} to τ_{p+} and η jumps from η_{p-} to η_{p+} . In the limit $\tau_0 \rightarrow 0$, $M \rightarrow \infty$, such a precursor shock always occurs, with $\tau_{p-} = 0$ and $\tau_{p+} \equiv \tau_p$, although the shock jump is small if $\bar{\theta} \gg 1$. If $\tau_0 > 0$, then there is a precursor shock only if $\bar{\theta}$ is small enough. For $\bar{\theta}$ smaller still, the precursor shock and the main shock merge into a single shock at which both density and temperature are discontinuous. For a strong shock ($M \rightarrow \infty$), this occurs for $\bar{\theta} < 4/3^{1/2}$ in the adiabatic case, and at a larger value of $\bar{\theta}$ is there is radiative cooling.

IV. APPROXIMATE ANALYTIC SOLUTIONS

In this section we derive simple analytic solutions that, given certain assumptions and approximations, describe various portions of the shock, and then use these to estimate the shock temperature. For simplicity we consider the limit of a very strong shock, with $\tau_0 \rightarrow 0$, $M \rightarrow \infty$, and also assume $\tau_c \ll 1$. We also assume that the thermal conductivity and cooling function are power laws in temperature: $l(\tau) = a\tau^\alpha$, $k(\tau) = b\tau^\beta$, so that $k(\tau)l(\tau) = ab\tau^{\alpha+\beta} \equiv c\tau^\gamma$, with $\gamma > 1$. We consider separately the ranges $\eta > \frac{1}{2}$ (+), upstream of the main shock, and $\eta < \frac{1}{2}$ (-), downstream of the main shock.

a) Behavior for $\frac{3}{4} \leq \eta \leq 1$ (Upstream)

Since $\tau_0 = 0$, the (+) range is restricted to $\frac{3}{4} \leq \eta \leq 1$, $\tau \leq \frac{3}{16}$. For $1 - \eta \ll 1$, we have

$$\tau \approx 1 - \eta \ll 1. \quad (4.1)$$

In this approximation, we have $\rho \approx \rho_0$, i.e., the flow is *isochoric*. Taking τ as our basic variable, we can rewrite equation (3.4) for $q = -|q|$ as

$$\frac{d|q|^2}{d\tau} - 6|q| \approx 2k(\tau)l(\tau) = 2c\tau^\gamma, \quad (4.2)$$

The saturated conductive flux is approximately

$$|q_{sat}| \approx 2\bar{\theta}\tau^{3/2} \quad (4.3)$$

and

$$f \approx 1 + 3\tau - |q|. \quad (4.4)$$

Equation (3.5) becomes

$$d\sigma/d\tau \approx d\xi/d\tau = -k(\tau)/q(\tau). \quad (4.5)$$

While strictly valid only for $1 - \eta \ll 1$, the above equations are roughly correct even for $\eta = \frac{3}{4}$.

If we neglect the effects of saturation, we find that the solution to equation (4.2), subject to the boundary condition $|q| = 0$ at $\tau = 0$, has limiting behaviors

$$\begin{aligned} |q| &\approx 3\tau, & \tau &\ll \left(\frac{9}{c}\right)^{1/(\gamma-1)}, \\ &\approx \left(\frac{2c}{\gamma+1}\right)^{1/2} \tau^{(\gamma+1)/2}, & \tau &\gg \left[\frac{9(\gamma+1)}{2c}\right]^{1/(\gamma-1)}. \end{aligned} \quad (4.6)$$

The large- τ behavior is physically relevant only if it occurs for $\tau \lesssim \frac{1}{4}$.

Now consider the effects of finite $\bar{\theta}$. Comparing equations (4.6) and (4.3), we find that q would always be saturated for $\tau \rightarrow 0$, if the solution were continuous. However, for $\tau_0 = 0$, $f_{+sat} > f_0$ in the range $0 < \tau < \tau_p$, so no continuous solution is possible in this range. For $\bar{\theta} < 4/3^{1/2}$, $\tau_p > 3/16$, and the solution jumps straight from $\eta = 1$, $\tau = 0$ to $\eta \leq \frac{1}{4}$. For $\bar{\theta} \gg 1$, $\tau_p \approx (3/2\bar{\theta})^2 \ll 1$, and the solution has a shock transition from $\tau = 0$ to $\tau = \tau_p$, after which it varies continuously over some range of τ , before undergoing a second shock transition, this one at constant temperature $\tau = \tau_s$, to the region $\eta < \frac{1}{4}$. Whether the conduction is saturated in the range $\tau_p < \tau < \tau_s$ depends on the value of

$$\Delta_+ \equiv \frac{d|q|_{unsat}}{d\tau} - \frac{d|q|_{sat}}{d\tau} = 3 + \frac{c}{2\bar{\theta}} \tau^{\gamma-3/2} - 3\bar{\theta}\tau^{1/2}, \quad (4.7)$$

Δ_+ being evaluated on the curve $q = q_{sat}$. For $\Delta_+ > 0$, the solution $q(\tau)$ may join the curve $q = q_{sat}$, while for $\Delta_+ < 0$, the solution must branch off. Thus, for $\gamma < 2$, q is unsaturated for $\tau \rightarrow \infty$, and for $\gamma > 2$, q is saturated for $\tau \rightarrow \infty$ but can be unsaturated at intermediate τ . Whether the regime " $\tau \rightarrow \infty$ " is reached in the physical range of τ depends on the values of c and $\bar{\theta}$.

b) Behavior for $0 \leq \eta \leq \frac{1}{4}$ (Downstream)

For $\tau_0 = 0$, the (-) range is restricted to $0 \leq \eta \leq \frac{1}{4}$, $\tau \leq 3/16$. For $\eta \ll 1$, we have

$$\tau \approx \eta \ll 1; \quad (4.8)$$

thus $p \approx \rho_0 v_0^2$, i.e., the flow is *isobaric*. Equation (3.4) approximates to

$$\frac{dq^2}{d\tau} + 10q \approx 2 \frac{k(\tau)l(\tau)}{\tau^2} = 2c\tau^{\gamma-2}, \quad (4.9)$$

while equation (3.6) becomes

$$q_{\text{sat}} \approx 2\bar{\theta}\tau^{1/2} \quad (4.10)$$

and

$$f \approx 5\tau + q; \quad (4.11)$$

$\xi(\tau)$ and $\sigma(\tau)$ can be found by integrating

$$\tau d\sigma/d\tau \approx d\xi/d\tau = -k(\tau)/q(\tau). \quad (4.12)$$

The above approximations are roughly valid even for $\eta = \frac{1}{4}$.

Consider the solution of equation (4.9) with boundary condition $q = 0$ at $\tau = 0$, i.e., $\tau_c = 0$. Solutions $q(\tau)$ for $\tau_c > 0$ converge on this solution from below. One finds the following limiting behaviors:

$$1 < \gamma < 3:$$

$$q \approx \left(\frac{2c}{\gamma-1}\right)^{1/2} \tau^{(\gamma-1)/2}, \quad \tau \ll \left[\frac{(\gamma-1)c}{50}\right]^{1/(3-\gamma)},$$

$$\approx \frac{1}{5} c\tau^{\gamma-2}, \quad \tau \gg \left(\frac{|\gamma-2|c}{25}\right)^{1/(3-\gamma)}, \left[\frac{(\gamma-1)c}{50}\right]^{1/(3-\gamma)}.$$

(4.13a)

$$\gamma = 3:$$

$$q = \frac{5}{2}[-1 + (1 + 4c/25)^{1/2}]\tau. \quad (4.13b)$$

$$\gamma > 3:$$

$$q \approx \frac{1}{5} c\tau^{\gamma-2}, \quad \tau \ll \left[\frac{25}{(\gamma-2)c}\right]^{1/(\gamma-3)},$$

$$\approx \left(\frac{2c}{\gamma-1}\right)^{1/2} \tau^{(\gamma-1)/2}, \quad \tau \gg \left[\frac{50}{(\gamma-1)c}\right]^{1/(\gamma-3)}.$$

(4.13c)

The solution for $\gamma = 3$ is exact. We see that for $\gamma < 3$, $q/f \approx 1$ at low temperatures and $q/f \ll 1$ at high temperatures, while for $\gamma > 3$, the reverse is true. For $\gamma = 3$, $q/f = \text{constant}$, independent of temperature in the downstream region.

Now consider the effects of saturation. Define

$$\Delta_- \equiv \frac{dq_{\text{unsat}}}{d\tau} - \frac{dq_{\text{sat}}}{d\tau} = -5 + \frac{c}{2\bar{\theta}} \tau^{\gamma-5/2} - \bar{\theta}\tau^{-1/2}. \quad (4.14)$$

For $\Delta_- > 0$, an unsaturated solution $q(\tau)$ can join onto $q = q_{\text{sat}}(\tau)$, while for $\Delta_- < 0$, the solution must branch off. Making use of this, and comparing the unsaturated solutions (4.13)–(4.10), one finds the following: for $1 < \gamma < 2$, $q(\tau)$ is saturated for $\tau \rightarrow 0$ and becomes unsaturated for $\tau \rightarrow \infty$; for $2 < \gamma < 5/2$, $q(\tau)$ is unsaturated for $\tau \rightarrow 0$ and unsaturated for $\tau \rightarrow \infty$, but can be saturated at intermediate τ ; for $\gamma > 5/2$, $q(\tau)$ is unsaturated for $\tau \rightarrow 0$ and becomes saturated for $\tau \rightarrow \infty$. The regime “ $\tau \rightarrow \infty$ ” may or may not be achieved in the physical range of τ , depending on the values of c and $\bar{\theta}$.

c) Determination of Shock Temperature and Spatial Structure

The shock temperature can be estimated by matching the approximate solutions for the upstream and downstream regions. We concentrate on the case $\alpha = \frac{1}{2}$, $\beta = 5/2$, $\gamma = 3$, because this turns out to be of the most physical interest (see § V). The case $\gamma = 3$ also happens to be the simplest to analyze.

Consider first the case in which saturation effects can be neglected. Here τ_s is found by solving $f_+(\tau) = f_-(\tau)$, with $f_+(\tau)$ given by equations (4.4) and (4.6), and $f_-(\tau)$ given by equations (4.11) and (4.13b). We find

$$\tau_s \approx \frac{\frac{2}{5}}{1 + (1 + 4c/25)^{1/2}} \quad (\gamma = 3), \quad (4.15)$$

and $f_+(\tau) \approx 1$ for $\tau \leq \tau_s$, so that only a negligible fraction of the total energy flux is radiated from the upstream region. Numerical integration of the exact equations shows that these approximate results are accurate to better than 10%. In the limit $c \rightarrow 0$ in which there is no thermal conduction, the approximate solution gives $\tau_s = \frac{1}{5}$, to be compared with the exact solution $\tau_s = 3/16$. Equation (4.15) for τ_s can be further approximated as

$$\tau_s \approx \frac{1}{5} \quad (c \lesssim 25, \gamma = 3),$$

$$\approx 1/\sqrt{c} \quad (c \gtrsim 25, \gamma = 3), \quad (4.16)$$

showing that the effects of conduction become significant for $c \gtrsim 25$, leading to a reduction in the shock temperature by a factor of $(25/c)^{1/2}$ compared with its value in the absence of conduction.

Given the approximate solutions for $q(\tau)$, one can then derive the dependence of temperature on position $\tau(\xi)$ by integrating equation (4.5) for $\xi < 0$, or equation (4.12) for $\xi > 0$ (we take $\xi = 0$ at the shock front). For $\xi < 0$, equation (4.6) gives $q \approx -3\tau$, and

$$\tau \approx \left(\tau_s^\beta + \frac{3\beta}{b} \xi\right)^{1/\beta} \quad (\xi < 0), \quad (4.17a)$$

while for $\xi > 0$, q is given by equation (4.13b) and

$$\tau \approx \left\{ \tau_s^\beta - \frac{5\beta}{2b} [(1 + 4c/25)^{1/2} - 1]\xi \right\}^{1/\beta} \quad (\xi > 0, \gamma = 3). \quad (4.17b)$$

We assume $\beta > 0$. We see that a conductive precursor propagates ahead of the shock by a distance $\xi_1 \approx -(b/3\beta)\tau_s^\beta$, while in the postshock region the gas cools back down to $\tau = 0$ in a distance $\xi_2 \approx (2b/5\beta)[(1 + 4c/25)^{1/2} - 1]^{-1}\tau_s^\beta$. Thus, compared with its value in the absence of conduction, the spatial thickness of the cooling layer behind the shock is changed by a factor $(25/c)^{(2-\alpha)/2}$ for $c \gtrsim 25$. One can derive similar relations with the column density σ instead of ξ as the independent variable. One finds that the column density of the precursor is $\sigma_1 \approx \xi_1$ (for $\beta > 0$), while that of the postshock cooling zone is $\sigma_2 \approx \beta/(\beta-1)(\xi_2/\tau_s)$ (for $\beta > 1$). Thus, for $c \gtrsim 25$, conduction changes the column density for cooling by a factor $(25/c)^{(1-\alpha)/2}$. The column density is reduced for $\alpha < 1$. This reduction occurs because the cooling rate per unit mass Λ/ρ , which is proportional to \bar{L}/\bar{T} in the approximately isobaric conditions behind the shock, increases with decreasing temperature if $\alpha < 1$. Therefore, conduction transports heat to parts of the shocked layer where it is radiated more efficiently. Similarly, the thickness of the cooling layer is reduced by conduction if $\alpha < 2$, because then the cooling rate per unit volume $\Lambda \propto \bar{L}/\bar{T}^2$ increases with decreasing temperature.

Now consider the effects of saturation. Rather than varying continuously, the temperature in the conductive precursor jumps from $\tau = 0$ to $\tau = \tau_p$ at a weak shock ahead of the main shock, where τ_p is the solution of $f_{+\text{sat}}(\tau) = 1$. For $\bar{\theta} \gg 1$, equations (4.3) and (4.4) give $\tau_p \approx (3/2\bar{\theta})^2$. If $\tau_p > \tau_s$, then the precursor

sor shock at τ_p and the main shock at τ_s merge into a single shock at τ_s ; using equation (4.16), we find that this occurs for all values of c for $\bar{\theta} \lesssim (3\sqrt{5})/2$, and at $c \gtrsim (2\bar{\theta}/3)^4$ for $\bar{\theta} \gtrsim (3\sqrt{5})/2$. For $\tau_p < \tau_s$, $\Delta_+ < 0$ at $\tau = \tau_p$ (eq. [4.7]), and the solution $f_+(\tau)$ is unsaturated for $\tau_p < \tau < \tau_s$. Since $f_+ \approx 1$ in this range, the solution differs negligibly from that derived above neglecting saturation. In the postshock region, saturation becomes important only at values of c large enough that the precursor does not exist. Combining equations (4.10) and (4.13b), we find that the conductive flux is saturated for $\tau > \tau_{\text{sat}}$, with $\tau_{\text{sat}} \approx \{4\bar{\theta}/5[(1 + 4c/25)^{1/2} - 1]\}^2$. If $\tau_{\text{sat}} < \tau_s$, then τ_s is found from $f_{\text{sat}}(\tau) = 1$. For $\bar{\theta} \lesssim (\sqrt{5})/2$, saturation sets in for $c \gtrsim (10\sqrt{5})\bar{\theta} < 25$, and $\tau_s \approx \frac{1}{5}$ in the saturated regime; for $\bar{\theta} \gtrsim (\sqrt{5})/2$, saturation sets in for $c \gtrsim (2\bar{\theta})^4 > 25$, and $\tau_s \approx 1/(2\bar{\theta})^2$ in the saturated regime. Thus for $\bar{\theta} \lesssim (\sqrt{5})/2$, saturation sets in before conduction can significantly affect the shock temperature.

We now briefly consider determination of the shock structure for $\gamma \neq 3$. The value of τ_s is found by equating the approximate solution for f given by equations (4.4) and (4.6) with that given by equations (4.11) and (4.13a) ($1 < \gamma < 3$) or (4.13c) ($\gamma > 3$). We find that $f \approx 1$ at the shock front is always valid, and

$$\tau_s \approx \frac{1}{5}, \quad c \lesssim c_{\text{crit}},$$

$$\approx \left(\frac{\gamma-1}{2c}\right)^{1/(\gamma-1)}, \quad c \gtrsim c_{\text{crit}}, \quad (4.18)$$

where $c_{\text{crit}} \sim 5\gamma^{-1}$. For $\gamma < 3$, conduction becomes significant first in low-temperature parts of the postshock region, while for $\gamma > 3$ conduction becomes significant first at $\tau = \tau_s$, and is always negligible at sufficiently low temperatures. The spatial structure of the precursor is the same as for $\gamma = 3$ (eq. [4.17a]). In the absence of conduction, the postshock cooling layer has finite thickness if $\alpha < 3$, and finite column density if $\alpha < 2$. With conduction, the cooling layer thickness ξ_2 is finite if in addition $\beta - \alpha + 3 > 0$, and is changed by a factor $\sim (c_{\text{crit}}/c)^{(2-\alpha)/(\gamma-1)}$ for $c > c_{\text{crit}}$, while the column density σ_2 is finite if $\beta - \alpha + 1 > 0$, and is changed by a factor $\sim (c_{\text{crit}}/c)^{(1-\alpha)/(\gamma-1)}$ for $c > c_{\text{crit}}$. As in the case $\gamma = 3$, we see that conduction reduces ξ_2 for $\alpha < 2$, and reduces σ_2 for $\alpha < 1$.

V. PHYSICAL EXAMPLE

We consider the structure of a strong radiative shock in which the gas is fully ionized. The conductive heat flux in a plasma is dominated by the electrons. Assuming that the electrons are scattered only by Coulomb interactions with ions and other electrons, the conductivity in the diffusive regime is

$$\kappa = 20 \left(\frac{2}{\pi}\right)^{3/2} \left(\frac{k_B^{7/2}}{m_e^{1/2} e^4}\right) \left(\frac{\epsilon \delta_T}{\bar{Z} \ln \Lambda_C}\right) T^{5/2} \quad (5.1)$$

(Spitzer 1962), where $\bar{Z} \equiv \sum n_i Z_i^2 / n_e$ is the mean ionic charge, and $\epsilon \delta_T$ is a function of \bar{Z} given approximately by $\epsilon \delta_T \approx 0.095(\bar{Z} + 0.24)/(1 + 0.24\bar{Z})$ (Max, McKee, and Mead 1980). The Coulomb logarithm is a slowly varying function of n_e , T , and Z for which I adopt the fixed value $\ln \Lambda_C = 32$. The saturation parameter $\bar{\theta}$ can be expressed as

$$\bar{\theta} = \epsilon \left(\frac{2}{\pi}\right)^{1/2} \left(\frac{m_H}{m_e}\right)^{1/2} \frac{\mu_e^{3/2}}{\mu_e} \quad (5.2)$$

(Cowie and McKee 1977), where μ_e is the mean molecular mass per electron. The value of the suppression factor ϵ' is somewhat

uncertain; I adopt Cowie and McKee's estimate $\epsilon' = 0.4$, although some plasma experiments suggest values as low as $\epsilon' \approx 0.04$ (Max, McKee, and Mead 1980).

The above estimates of the conductive parameters neglect the effects of magnetic fields and plasma turbulence, which both tend to suppress thermal conduction. Thus the calculations in this paper give upper limits on the effectiveness of conduction. The effect of magnetic fields on thermal conduction is discussed by Balbus (1986). Even quite a weak field will inhibit particle motion perpendicular to the field direction. If the magnetic field is uniform and makes an angle ϕ with the flow direction, the heat flux in this direction is then reduced by a factor $\cos^2 \phi$ in the diffusive regime and $\cos \phi$ in the saturated regime. If the field is tangled, the suppression factor may be larger. If the plasma is turbulent, particles will be scattered by plasma waves, reducing the mean free path and thus the conductivity. A likely source of turbulence is the shock front itself: as discussed by McKee and Hollenbach (1980), in the low-density plasmas characteristic of astrophysics, the collisionless plasma scales (Debye length, Larmor radius) are typically much smaller than the Coulomb collision length, so that thermalization of particle velocities in the shock front is accomplished by plasma turbulence rather than by collisions. There will be a turbulent layer at the shock front in which the particle mean free path is comparable to collisionless scales (Tidman and Krall 1971), so that the conductivity is reduced far below the value given by equation (5.1). However, the thickness of this layer is also expected to be comparable to collisionless scales. If this layer is thin compared with the other scales in the problem, then the shock jump conditions will correctly relate quantities on either side of the layer, where the equations of this paper do apply, and the analysis of the structure of the rest of the shock wave goes through unchanged.

In a fully ionized plasma, the radiation is dominated by bremsstrahlung, for which

$$\Lambda_B = \left(\frac{16}{3}\right) \left(\frac{2\pi}{3}\right)^{1/2} \left(\frac{k_B^{1/2} e^6}{m_e^{3/2} \hbar C^3}\right) \bar{g}_B \bar{Z} n_e^2 T^{1/2} \quad (5.3)$$

(e.g., Karzas and Latter 1961), where C is the velocity of light. The average Gaunt factor \bar{g}_B is very weakly varying; I adopt a constant value $\bar{g}_B = 1.3$.

For conduction and cooling rates given by equations (5.1) and (5.3), we have $\alpha = \frac{1}{2}$, $\beta = 5/2$, $\gamma = 3$, and

$$c = \left(\frac{5 \times 2^{10}}{3^{3/2} \pi}\right) \left(\frac{m_H}{m_e}\right)^2 \left(\frac{e^2}{\hbar C}\right) \left(\frac{\bar{g}_B \epsilon \delta_T}{\ln \Lambda_C}\right) \frac{\mu^4}{\mu_e^2} \left(\frac{v_0}{C}\right)^2. \quad (5.4)$$

The analysis of § IV shows that, for $\gamma = 3$, conduction significantly affects the shock structure for $c \gtrsim 25$. This critical value of c corresponds through equation (5.4) to a critical value $v_{0 \text{ crit}}$ of the shock velocity, and to a critical value of the shock temperature $T_{s \text{ crit}} \approx (\mu m_H / 5 k_B) v_{0 \text{ crit}}^2$. The values of $v_{0 \text{ crit}}$ and $T_{s \text{ crit}}$ have a significant dependence on the composition of the plasma. For simplicity consider a plasma containing a single species with atomic number Z and mass number A , so that $\mu = A/(Z+1)$ and $\mu_e = A/Z$. Then we find for hydrogen ($Z = 1$, $A = 1$) $v_{0 \text{ crit}} \approx 3.5 \times 10^4 \text{ km s}^{-1}$, $T_{s \text{ crit}} \approx 1.5 \times 10^{10} \text{ K}$; for helium ($Z = 2$, $A = 4$) $v_{0 \text{ crit}} \approx 8.0 \times 10^3 \text{ km s}^{-1}$, $T_{s \text{ crit}} \approx 2.0 \times 10^9 \text{ K}$; for oxygen ($Z = 8$, $A = 16$) $v_{0 \text{ crit}} \approx 3.3 \times 10^3 \text{ km s}^{-1}$, $T_{s \text{ crit}} \approx 4.6 \times 10^8 \text{ K}$. For solar composition, $v_{0 \text{ crit}} \approx 2.6 \times 10^4 \text{ km s}^{-1}$, $T_{s \text{ crit}} \approx 1.0 \times 10^{10} \text{ K}$, not much different from the values for hydrogen. This composition dependence is dominated by that of the mean molecular mass μ . For the same

compositions, the saturation parameter has values $\bar{\theta} = 4.8$ (H), $\bar{\theta} = 10.6$ (He), $\bar{\theta} = 16.2$ (O) and $\bar{\theta} = 5.6$ (solar). We see from the results of § IV that at low enough shock velocities, the shock will have a conductive precursor, and that conduction will have an important effect on the shock temperature before saturation sets in.

The above analysis neglects contributions to the cooling rate from line and recombination radiation, which become important when the plasma is only partially ionized. For a plasma of solar composition in ionization equilibrium, line and recombination radiation exceed bremsstrahlung for $T \lesssim 10^7$ K. Increased cooling tends to make conduction more important, because it steepens the temperature gradient in the postshock region. I performed numerical integrations of the exact equations for the shock structure using the analytic fit to the solar abundance equilibrium cooling curve given by Rosner, Tucker, and Vaiana (1978) for the range 1.4×10^4 K $< T < 4.7 \times 10^7$ K, with bremsstrahlung at the rate given by equation (5.3) at higher temperatures, and the cooling rate set to zero at lower temperatures. These calculations show that the estimate made above for the shock velocity at which conduction has a significant effect on the shock temperature and thickness remains valid, even including these extra contributions to the cooling rate.

When radiative cooling is by bremsstrahlung alone, the *local* structure of the postshock region is nowhere significantly affected by conduction unless the *global* structure is. This result is no longer true when line and recombination cooling are included. A useful measure of the effect of conduction on the *local* structure is the ratio $d\Sigma_c/d\Sigma_n \equiv (d\Sigma_c/dT)/(d\Sigma_n/dT)$, $d\Sigma_c/dT$ being the column density per unit temperature in the postshock region with conduction, and $d\Sigma_n/dT$ being the column density per unit temperature without conduction, evaluated at the same temperature. The ratio $d\Sigma_c/d\Sigma_n$ was evaluated for the shock structure calculations using the solar abundance cooling curve; the deviations from unity were found to be largest at the cutoff in the cooling function at $T_c = 1.4 \times 10^4$ K, and at the peak of the cooling curve at $T \sim 10^5$ K. At the cooling cutoff, we have formally $d\Sigma_c/d\Sigma_n \rightarrow \infty$. This is because, if $L(T)$ goes to zero discontinuously at $T = T_c$, $x = x_c$, then in the absence of conduction, $(T - T_c) \propto (x - x_c)$ for $x < x_c$ and $T = T_c$ for $x > x_c$, in the neighborhood of the cutoff, so that dT/dx is discontinuous; when conduction is included, the behavior is $(T - T_c) \propto (x - x_c)^2$ for $x < x_c$, so that dT/dx goes to zero continuously, avoiding the divergence in the conductive flux that would otherwise arise. These effects of the sharp cutoff on $d\Sigma_c/d\Sigma_n$ are confined to the neighbourhood $T \sim T_c$. The deviations of $d\Sigma_c/d\Sigma_n$ from unity at the peak of the cooling curve increase with the shock velocity: they are only a few percent for $v_0 = 10^2$ km s $^{-1}$, they reach a factor of 2 at $v_0 \approx 10^3$ km s $^{-1}$, and they reach a factor of 10 at $v_0 \approx 5 \times 10^3$ km s $^{-1}$. These results are not affected by saturation unless $\bar{\theta}$ is smaller than $\sim 10^{-2}$ of the value estimated above.

A further effect on the radiative cooling rate would be possible departures from ionization equilibrium. Raymond (1979) and Shull and McKee (1979) find that this is an important effect for shock velocities $v_0 \approx 100$ km s $^{-1}$ (for solar abundances), for which subequilibrium ionization of hydrogen and helium may cause the cooling rate in the immediate postshock region to exceed the equilibrium value by a factor of 10 or more. This effect should become small at larger shock velocities, because ionization of these elements becomes nearly

complete. To estimate the effects of enhanced cooling, I calculated shock models using the solar abundance cooling function mentioned above, but with the nonbremsstrahlung part of the cooling rate arbitrarily boosted by a factor of 10. This could alternatively represent the effects of increasing the heavy-element abundance by a factor of 10 above solar. The deviations of $d\Sigma_c/d\Sigma_n$ from unity near the peak of the cooling curve are now about 10% for $v_0 = 10^2$ km s $^{-1}$, increasing to a factor of 2 for $v_0 \approx 3 \times 10^2$ km s $^{-1}$ and a factor of 10 for $v_0 \approx 2 \times 10^3$ km s $^{-1}$. However, the effect of conduction on the shock temperature is only a few percent even at $v_0 = 10^4$ km s $^{-1}$. In all of the numerical calculations, $f \approx 1$ at the shock front was found to be a good approximation.

For the case in which the cooling function $\bar{L}(\bar{T})$ and/or the conductivity $\bar{\kappa}(\bar{T})$ are not power laws in \bar{T} , one can estimate the shock velocity at which conduction significantly affects the shock temperature as follows (we assume a strong shock): in the absence of conduction, the characteristic length scale for radiative cooling in the postshock region is $x_{\text{cool}} = (9/512)(v_0^3/\rho_0 \bar{L}_s)$, where \bar{L}_s is evaluated at the temperature $\bar{T}_s = (3/16)v_0^2$. The conductive heat flux is then $Q \sim \bar{\kappa}_s \bar{T}_s/x_{\text{cool}}$. Conduction is expected to become important when this conductive flux becomes comparable to the total energy flux $F_0 = \frac{1}{2}\rho_0 v_0^3$. The condition $|Q|/F_0 = 1$ gives $\bar{\kappa}_s \bar{L}_s/v_0^4 = 3/64$. For power-law conductivity and cooling functions, this gives almost the same critical shock velocity as the results of § IV.

Finally, we consider relativistic corrections, which become important at high temperatures. The electrons become relativistic for $T \gtrsim m_e c^2/k_B \approx 6 \times 10^9$ K. This has several effects. At given electron and ion densities, the expressions for the conductivity and bremsstrahlung cooling rate in the extreme relativistic regime ($k_B T \gg m_e c^2$) differ from the nonrelativistic expressions by factors $\sim 2(m_e c^2/k_B T)^{1/2}$ and $\sim 3(k_B T/m_e c^2)^{1/2}$, respectively (Lifshitz and Pitaevskii 1981; Bisnovatyi-Kogan, Zeldovich, and Sunyaev 1971), so that $\bar{\kappa}\bar{L}$ has the same temperature dependence but is somewhat larger. Another effect is the creation of electron-positron pairs, which boosts the thermal energy density and cooling rate at given temperature and baryon density. If pair creation in the shock is significant, the results presented here would have to be modified.

VI. SUMMARY

This paper presents a general procedure for deriving the structure of a steady state, plane-parallel shock in which both thermal conduction and radiative cooling are important. The gas is assumed to behave as a single fluid with perfect-gas equation of state. Conduction in both diffusive and saturated regimes is treated. In the case in which $\kappa = \kappa(T)$ and $\Lambda = \rho^2 \bar{L}(T)$, the solutions scale with the preshock density ρ_0 as $\rho \propto \rho_0$, $x \propto 1/\rho_0$, $T = \text{constant}$, x being the spatial coordinate. For a $\gamma = 5/3$ gas, the condition for a shock to occur is $M > 3/\sqrt{5}$ with diffusive conduction and no radiation, while if radiative cooling is effective, shocks can occur for $M > 1$, where M is the adiabatic Mach number. When combined with radiative cooling, conduction has the effect of reducing the shock temperature at a given shock velocity. If conduction is everywhere in the diffusive regime, then the temperature varies continuously, even at shocks, but this need no longer be true if the saturation parameter $\bar{\theta}$ is finite. If there is a shock with finite M , then if $\bar{\theta}$ is sufficiently large the shock is isothermal and is preceded by a conductively heated precursor in which temperature varies smoothly. If $\bar{\theta}$ is reduced, a "precursor"

shock, across which there is a temperature jump, develops ahead of the "main shock." If $\bar{\theta}$ is made even smaller, the precursor shock merges with the main shock. For a strong shock ($M \rightarrow \infty$) this occurs (and the precursor vanishes entirely) for $\bar{\theta} < 4/\sqrt{3}$ if there is no radiative cooling, and at larger values of $\bar{\theta}$ if there is cooling.

For a strong shock, with $M \gg 1$, the pre-(main) shock flow is at roughly constant density, while the post-(main) shock flow is at roughly constant pressure. These features allow approximate analytical solutions to be derived, when one makes the additional assumptions that the conductivity and cooling rate have power-law dependences on temperature. These analytical results, together with numerical calculations, are used to investigate shock wave structure for realistic conductivity and cooling laws, assuming no suppression of conduction by magnetic fields. For an ionized gas of solar composition, conduction is found to have a significant effect on the shock

temperature and overall thickness of the postshock region only for shock velocities $v_0 \gtrsim 3 \times 10^4 \text{ km s}^{-1}$, corresponding to shock temperatures $T_s \gtrsim 10^{10} \text{ K}$. However, conduction can have significant effects on the local structure of the shock wave, in particular the column density per unit temperature $d\Sigma/dT$, at much lower velocities: for solar composition, these effects are of order unity at $T \sim 10^5 \text{ K}$, corresponding to the peak of the cooling curve, for $v_0 \approx 10^3 \text{ km s}^{-1}$. The effects of conduction are also greatly enhanced if the gas contains a large proportion of heavy elements. In all cases investigated, the radiation from the conductive precursor was found to be a negligible fraction of the total.

I thank S. Balbus and G. B. Field for useful discussions, and the referee for helpful suggestions. This research was supported by a SERC Postdoctoral Research Fellowship and by National Aeronautics and Space Administration grant NAGW-931.

REFERENCES

- Balbus, S. A. 1986, *Ap. J.*, **304**, 787.
 Bisnovatyi-Kogan, G. S., Zel'dovich, Ya. B., and Sunyaev, R. A. 1971, *Soviet Astr.—AJ*, **15**, 17.
 Bond, J. R., Centrella, J., Szalay, A. S., and Wilson, J. R. 1984, *M.N.R.A.S.*, **210**, 515.
 Chevalier, R. A. 1975, *Ap. J.*, **198**, 355.
 Cowie, L. L. 1977, *Ap. J.*, **215**, 226.
 Cowie, L. L., and McKee, C. F. 1977, *Ap. J.*, **211**, 135.
 Doroshkevich, A. G., and Zel'dovich, Ya. B. 1981, *Soviet Phys.—JETP*, **53**, 405.
 Karzas, W. J., and Latter, R. 1961, *Ap. J. Suppl.*, **6**, 167.
 Landau, L. D., and Lifshitz, E. M. 1959, *Fluid Mechanics* (Oxford: Pergamon).
 Lifshitz, E. M., and Pitaevskii, L. P. 1981, *Physical Kinetics* (Oxford: Pergamon).
 Max, C. E., McKee, C. F., and Mead, W. C. 1980, *Phys. Fluids*, **23**, 1620.
 McKee, C. F., and Cowie, L. L. 1977, *Ap. J.*, **215**, 213.
 McKee, C. F., and Hollenbach, D. J. 1980, *Ann. Rev. Astr. Ap.*, **18**, 219.
 Penston, M. V., and Brown, F. E. 1970, *M.N.R.A.S.*, **150**, 373.
 Raymond, J. C. 1979, *Ap. J. Suppl.*, **39**, 1.
 Rosner, R., Tucker, W. H., and Vaiana, G. S. 1978, *Ap. J.*, **220**, 643.
 Shapiro, P. R., and Struck-Marcell, C. 1985, *Ap. J. Suppl.*, **57**, 205.
 Shull, J. M., and McKee, C. F. 1979, *Ap. J.*, **227**, 131.
 Spitzer, L. 1962, *Physics of Fully Ionized Gases* (2d ed.; New York: Interscience).
 Tidman, D. A., and Krall, N. A. 1971, *Shock Waves in Collisionless Plasmas* (New York: Wiley).
 Zel'dovich, Ya. B., and Raizer, Yu. P. 1967, *Physics of Shock Waves and High Temperature Phenomena*, Vols. 1 and 2 (New York: Academic).

CEDRIC G. LACEY: Center for Astrophysics, MS 51, 60 Garden Street, Cambridge, MA 02138